IET Generation, Transmission & Distribution

Research Article

IET Journals
The Institution of Engineering and Technology

Algorithm for load cycling correction to minimise the dry zone influences on the cross-linked polyethylene (XLPE) cable insulation

ISSN 1751-8687
Received on 2nd March 2020
Revised 12th June 2020
Accepted on 29th June 2020
E-First on 14th September 2020
doi: 10.1049/iet-gtd.2020.0406
www.ietdl.org

Osama E. Gouda[1] ✉, *Gomaa F.A. Osman*[2]

[1]*Faculty of Engineering, Cairo University, Giza, Egypt*
[2]*Benha Faculty of Engineering, Benha University, Benha, Egypt*
✉ *E-mail: prof_ossama11@yahoo.com*

Abstract: Dry zone formation around underground power cables during load cycling may lead to thermal failure of the cable's insulation. This phenomenon has to be recorded to send an alarm to the maintenance crew when the soil around the cable reaches the critical value at which the dry zone has started to be formed. In this study, the buried cable thermal model is modified to include occurrences of dry band formation during dynamic loading. An algorithm has been proposed for corrections of the cable load cycle to maintain the insulation maximum temperature at 85°C and not exceed this limit. This is suggested for reducing the dry zone formation effect on the cable insulation lifetime. The study is done on different single-core cables using different soil samples that can be used as backfill materials. The variations in thermal soil resistivity and soil thermal capacitance with temperature and moisture content of backfill soil are considered. The practical system used for monitoring the dry zone formation around the cable has been proposed.

1 Introduction

The use of underground power cables (UGPCs) for electrical energy transmission and distribution in towns and compactly populated zones is growing every year. Thermal analysis of UGPCs is a subject, which has received extensive courtesy in current years. UGPC is highly expensive compared to overhead lines in most instances. Cable current carrying capacity calculation involves knowing numerous issues such as the cable construction, ambient condition, the buried method under the ground surface and the soil thermal characteristics as specified in IEC 60287-1-3 [1]. The combination of all these factors may reduce steady-state capacity of UGPCs up to 40% of its rated capacity [2–4]. The cyclic current loading of UGPC changes from time to time depending on the load nature. The cyclic loading current generates heat dissipating to the surrounding soil and changes the moisture content and the soil temperature. The soil temperature increase causes the moisture content to migrate and there will be dry zone formation in the surrounding soil. This leads to an increase in the soil thermal resistivity and slow rate of heat dissipation from the cable to the surrounding soil [5–11]. Increasing conductor and insulation temperatures lead to the decrease of the current rating of the cable, since the UGPC conductor temperature is limited by the insulating material type [12, 13].

The thermal analysis of UGPCs is discussed by many researchers using theoretical and experimental methods [3–20]. IEC 60853-2 [21] provides a method for determining transient temperature, but unfortunately, this standard ignores the possibility of dry band formation around the UGPC. Olsen *et al.* [22] discussed the transient temperature estimation during cyclic loading based on the thermoelectric method. Freitas *et al.* [23] used a numerical model for the thermal analysis of distribution UGPCs with constant and cyclic currents in the presence of moisture migration in the surrounding soil. Maximov *et al.* [24] presented an analytical model to estimate the current-carrying capacity of UGPCs. Zarchi *et al.* [25] proposed a thermal model to calculate cable transient temperature of UGPCs in a concrete duct bank. Carlos *et al.* [26] suggested a mathematical model of UGPC to calculate the temperature and capacity under steady-state and emergency conditions using finite difference method. Anders and El-Kady [27] performed the UGPC transient calculations based on the lumped parameter model of underground cable. Similar studies were done by Campbell *et al.* [28], Koopmans and Gouda [29], Anders and Radhakrishna [30] and Donazzi *et al.* [31] used Philip and De-Vries model equations [32] to include the transportation of moisture and heat of the soil with hysteretic moisture potential due to dynamic loading of the cable. It is known that there is an increase in the vapour flow in the soil surrounding the cable due to temperature rise. The vapour condensates in low-temperature zone far away from the surrounding cable route to be water. Actually, as the load decreases, the associated temperature also decreases, but this will not allow the lost moisture to come back around the cable in the form of water, instead it leaks in other places depending on the nature of the area surrounding the cable route, assuming there is no other source of water feeding the cable route.

The main contribution of this paper is to suggest an algorithm to correct the buried cable load cycle before insulation failure. For that modified thermal model of the cable and surrounding soil including the occurrence of dry band formation during dynamic loading is used for the emendation of the cable load cycle to maintain the insulation maximum temperature at 85°C and not exceed this limit and to reduce the dry zone formation effect on the cable insulation lifetime. The study is done on different single-core cables using different soil samples that can be used as backfill materials to correct the cables load cycles before reaching the thermal failure.

2 Experimental testing

2.1 Experimental arrangement of the thermal test

Experimental thermal tests have been implemented on eight soils. Each soil composition contains an amount of sand and another of clay beside an amount of moisture content as follows:

Sample (1) contains 90% sand + 10% clay by weight + 0.032 moisture content (m^3/m^3).

Sample (2) contains 80% sand + 20% clay by weight + 0.042 moisture content (m^3/m^3).

Sample (3) contains 70% sand + 30% clay by weight + 0.05 moisture content (m^3/m^3).

Sample (4) contains 60% sand + 40% clay by weight + 0.061 moisture content (m^3/m^3).

Sample (5) contains 50% sand + 50% clay by weight + 0.071 moisture content (m^3/m^3).

Sample (6) contains 50% sand + 50% clay by weight + 0.071 moisture content (m^3/m^3).

Sample (7) contains 30% sand + 70% clay by weight + 0.13 moisture content (m^3/m^3).

Sample (8) contains 15% sand + 85% clay by weight + 0.2 moisture content (m^3/m^3).

Each sample of soil is tested in a plastic cylinder of 120 mm height and 100 mm diametre as given in Fig. 1*a*. The simulation of UGPCs losses is done by heat produced by heater placed, at the top of the soil-testing device. The generated heat is measured by using, heat flux meter. The plastic cylinder contains the soil mixture, which is insulated from the surrounding by O-ring.

The temperature of the tested soil is measured by using K thermo-couples. It can accurately measure the temperatures in the range from − 270°C to 137°C with errors within 0.5–2°C. *K* thermo-couples has a sensitivity of 41 μV/°C. A number of thermocouples are placed along the length of the plastic cylinder. The moisture content is measured by using a moisture sensor within the plastic cylinder device. During experimental thermal tests, the heater is adjusted to produce 730 W/m^2 heat flux.

The suction tension is controlled to be infinity ($p_f = \infty$). It is one important factor affecting the thermal soil resistivity and dry zone formation around UGPCs. The suction tension is the soil water retention capacity by means of gravity, the soil water suction tension versus the degree of saturation is called p_f curve [29, 30]. It is described by the moisture potential of the soil in a water tube given in Figs. 1*a* and *b*. The importance of this factor is attributed to its influence on the thermal soil resistivity and dry band formation around UGPC. The thermal resistivity of each soil under testing is measured at infinity suction tension.

Heat flux distribution in the soil at actual cable loading is different from tested plastic cylinder condition, but to obtain each soil characteristic it has to be tested under uniform heat flux distribution which is carried out by the soil-testing device given in Fig. 1*a*. The test arrangement is given in Fig. 1*b* consists of soil-testing device, auto-transformer which is used to step down the AC input voltage from 220 V to a range between 45 and 50 V to supply the heater, DC power supply to give the required DC voltage to the moisture sensor and the output voltage of this device is set to be 12 V. Programmable logic controller (PLC) device is used to monitor and store the data of the thermocouples and moisture sensor. The used PLC unit is SIEMENS sector Simatic 300 Station type, its central processing unit is CPU312IFM, its power supply unit is PS307 2A and the analogue input module range is from 0 to 10 V. Computer unit consists of processor intel(R) Core(TM) i3-2328M CPU @ 2.20 GHz, installed memory (RAM) 4 GB and system type 64-bit operating system.

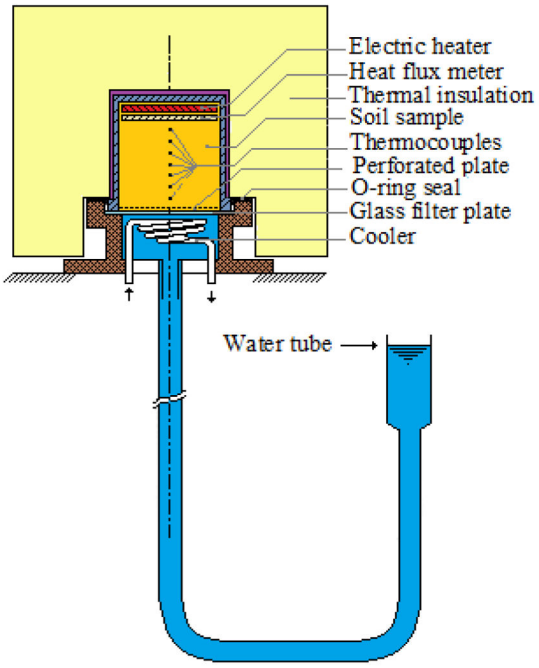

a

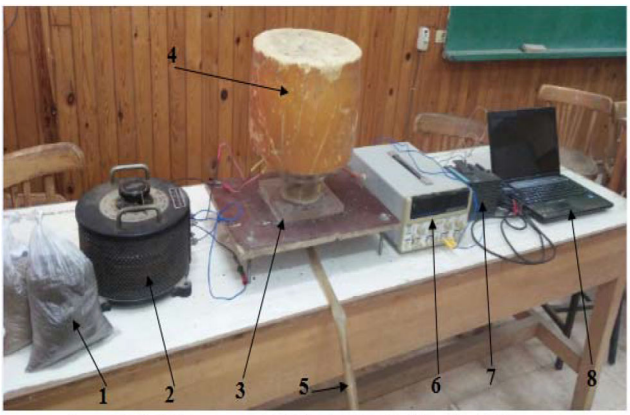

b

Fig. 1 *Experimental testing system*
(a) Soil-testing device, ***(b)*** Testing arrangement

2.2 Experimental results

The thermal characteristics of the tested soil are given in Table 1. From this table it is noticed that the time required for the dry zone formation decreases with the increase in the percentage of clay until the concentration reaches 50–60% of the soil content, after that, it increases again. This may be due to retainment the water and vapour by the clay.

One aim of the experimental tests is to obtain the relationship between the changes in the soil moisture content and its temperature variation. The following relation is obtained by the curve fitting of moisture content versus temperature measurements done on each soil sample as given in Fig. 2*a* with the estimated error of ± 1%

$$G_1 = K_1 + \frac{K_2 - K_1}{1 + \left(\frac{\theta}{K_3}\right)^{K_4}} \tag{1}$$

G_1 is the soil moisture content, θ is the temperature of the tested soil and K_1–K_4 are constants given in Table 2. The specific heat of each tested soil sample as a function of the soil temperature is given in (2). This relation is obtained by curve fitting of volumetric specific heat versus temperature measurements done on each soil sample as given in Fig. 2*a* with the estimated error of ± 2%

$$C_{\text{psoil}} = K_5 + \frac{K_6 - K_5}{1 + \left(\frac{\theta}{K_7}\right)^{K_8}} \tag{2}$$

Table 1 Tested soil samples properties by using 730 w/m^2 heat density and infinity suction tension

Soil No.	Time to form dry zone, h	Dry density, Kg/m^3	Wet thermal resistivity, ºC m/W	Critical temperature, ºC	Dry thermal resistivity, ºC m/W
1	2.5	1600	0.91	58	2.65
2	2.84	1567	0.847	56.5	2.85
3	2.33	1542	0.821	55.5	3.1
4	2	1502	0.818	54	3.5
5	1.83	1480	0.805	52	3.75
6	1.84	1445	0.794	51	4.2
7	2.17	1405	0.773	50	4.6
8	2.5	1375	0.746	49	0.92

C_{psoil} is the soil volumetric specific heat in (J/m^3 °C) and K_5–K_8 are constants for each soil sample given in Table 2. Fig. 2*c* gives the soil specific heat versus the soil moisture content graphs.

The general equation of the thermal resistivity ρ_{soil} as a function of the surrounding soil change with moisture content, temperature and the soil dry density is reported by Donazzi *et al*. [31]

$$\log_{10}\rho_{\text{soil}} = (g_1 - g_2\gamma_{\text{d}})x_1(\theta) + \frac{g_3}{g_4 + (G_1/x_2(\theta))} \tag{3}$$

where

$$x_1(\theta) = 1 + \frac{g_5(\theta - \theta_{\text{a}})}{(\gamma_{\text{d}} - \gamma_{\min})} + g_6(\gamma_{\max} - \gamma_{\text{d}})(\theta - \theta_{\text{a}})^2$$

$$x_2(\theta) = (1 - g_7(\theta - \theta_{\text{a}}))\frac{\gamma_{\text{d}}}{\gamma_{\text{w}}}$$

where $\gamma_{\max}$, $\gamma_{\min}$ and γ_{d} are the maximum, minimum and dry density of the soil, respectively, θ_{a} and θ are the ambient and soil temperature, respectively, and the values of g_1–g_7 are given as following [31]:

$$g_1 = 1.35 \quad g_3 = 0.017 \quad g_5 = 0.299 \quad g_7 = 0.01$$
$$g_2 = 1.15 \times 10^{-3} \quad g_4 = 0.0179 \quad g_6 = 1.08 \times 10^{-7}$$

The measurements indicate that the critical temperature to form a dry zone of different tested backfill samples changes from 49 to 58°C as given in Table 1. This is in good agreement with the results achieved by Gouda and El Dein [5].

3 Load cycling correction algorithm with respect to dry zone formation

The equivalent thermal model of UGPCs circuit is given in Fig. 3*a*. In this model T_1, T_3 and T_4 are the insulation, jacket and surrounding soil thermal resistances, respectively, and θ_e, θ_{s} and θ_{c} are the jacket, screen and conductor temperatures above ambient temperature θ_{a}, respectively. Q_{j}, Q_{s}, Q_{i}, Q_{c} and Q_{soil} are the thermal capacitances of the jacket, screen, insulation, conductor and surrounding soil, respectively, and p, p' are van wormer coefficients [21]. W_{c}, W_{s} and W_{d1} and W_{d2} are the losses of the conductor, sheath and dielectric of insulation layers. IEC 60287-1-3 standard is used to calculate the cable losses [1].

The thermal model of single-core UGPCs buried in the flat formation (step response) is reported by IEC 60853-2 [21], this reduced the cable circuit given in Fig. 3*a* into two loops as shown in Fig. 3*b*. One contains thermal capacitance of the conductor and inner part of the insulation thermal resistance and capacitance (T_A, Q_A) and the second loop contains the thermal capacitance and resistance of the cable of other layers (T_B, Q_B), which are given as follows:

$$T_A = T_1 \tag{4}$$

$$T_B = q_{\text{s}}T_3 \tag{5}$$

$$Q_A = Q_{\text{c}} + pQ_{\text{i}} \tag{6}$$

$$Q_B = (1 - p)Q_{\text{i}} + \frac{Q_{\text{s}} + p'Q_{\text{j}}}{q_{\text{s}}} \tag{7}$$

$$p = \frac{1}{2\ln\left(\frac{D_{\text{i}}}{d_{\text{c}}}\right)} - \frac{1}{\left(\frac{D_{\text{i}}}{d_{\text{c}}}\right)^2 - 1} \tag{8}$$

$$p' = \frac{1}{2\ln\left(\frac{D_e}{D_{\text{s}}}\right)} - \frac{1}{\left(\frac{D_e}{D_{\text{s}}}\right)^2 - 1} \tag{9}$$

$$M_o = \frac{1}{2}(Q_A\{T_A + T_B\} + Q_BT_B) \tag{10}$$

$$N_o = Q_AT_AQ_BT_B \tag{11}$$

$$a = \frac{M_o + \sqrt{M_o^2 - N_o}}{N_o} \tag{12}$$

$$b = \frac{M_o - \sqrt{M_o^2 - N_o}}{N_o} \tag{13}$$

$$T_{\text{a}} = \frac{1}{a - b}\left[\frac{1}{Q_A} - b(T_A + T_B)\right] \tag{14}$$

$$T_b = T_A + T_B - T_{\text{a}} \tag{15}$$

where q_{s} is the loss factor of the screen, M_o and N_o are coefficients used in the calculation of the cable thermal response as given in IEC 60853-2 and d_{c}, D_{i}, D_{s} and D_e are the external diametre of the conductor, insulation, screen and the cable surface, respectively. The dynamic conductor temperature (θ_{ce}) rise above the surface temperature is reported by IEC 60853-2 [21] as follows:

$$\theta_{ce}(t) = W_{\text{c}}\left[T_{\text{a}}(1 - \text{e}^{-\text{a}t}) + T_b(1 - \text{e}^{-bt})\right] \tag{16}$$

$$\theta_e(t) = \frac{\rho_{\text{soil}}W_{\text{I}}}{4\pi}\left\{\left[-\text{Ei}\left(\frac{-D_e^2}{16t\delta}\right) - \left[-\text{Ei}\left(\frac{-L^2}{t\delta}\right)\right]\right] + \sum_{K=1}^{K=N-1}\left[-\text{Ei}\left(\frac{-(d_{pk})^2}{4t\delta}\right) - \left[-\text{Ei}\left(\frac{(d'_{pk})^2}{4t\delta}\right)\right]\right]\right\} \tag{17}$$

The cable environment is the other part of the thermal model given by IEC 60853-2. The dynamic temperature of the centre cable surrounding (θ_e) rise above ambient temperature is determined by exponential integral (Ei) as given in (18) [21] where –Ei(−x) is the exponential integral, δ is the thermal diffusivity of the soil and W_{I} is the cable total power losses calculated according to the IEC 60287-1-3 [1]. d_{pk} and d′$_{pk}$ are the distances from the centre of cable (k) to the centre of cable (p) and distance from the image of the centre of cable (k) to the centre of cable (p), respectively and N

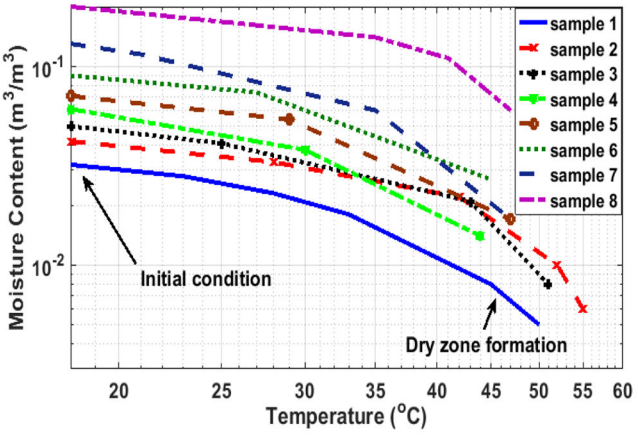

a

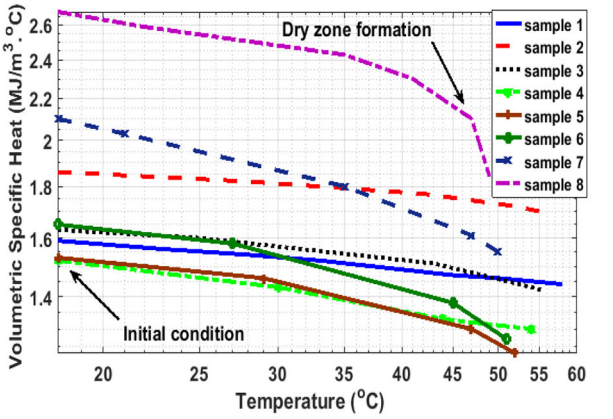

b

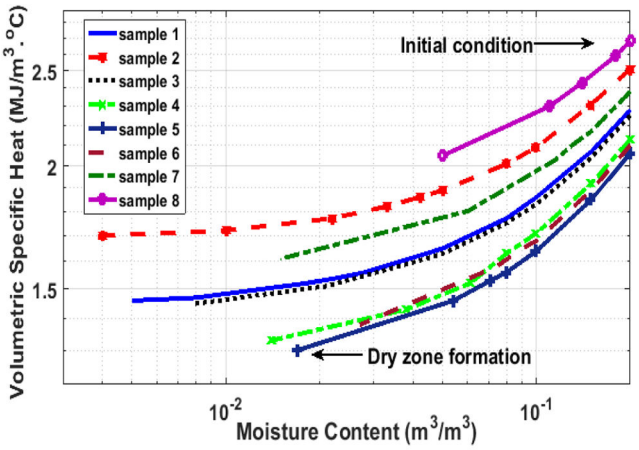

c

Fig. 2 *Results of experimental thermal tests*
(a) Relation between moisture content and soil temperature, ***(b)*** Relation between volumetric specific heat and soil temperature, ***(c)*** Soil specific heat versus the soil moisture content

is cable number. The total conductor transient temperature (θ_c) rise above ambient temperature is given as [21]

$$\theta_c(t) = \theta_{ce}(t) + \alpha(t)\,\theta_e(t) \tag{18}$$

Here, $\alpha(t)$ is the attainment factor used to control how the conductor temperature is affected by the surface temperature [21]

$$\alpha(t) = \frac{\theta_{ce}(t)}{[W_c(T_A + T_B)]} \tag{19}$$

As it is noticed from the above equations, EC 60853-2 method [21] ignored the moisture migration and temperature rise effects on the soil thermal resistivity and volumetric specific heat of the

Table 2 Constants of (1) and (2)

Soil sample	K_1	K_2	K_3	K_4
sample 1	−0.0181	0.0392	41.744	2.32
sample 2	−21705.9	0.045	30412.18	2.086
sample 3	−23,575.82	0.0584	161,771.8	1.62
sample 4	−0.077	0.0843	51.3	1.7
sample 5	−27,917.97	0.0804	35,265.32	1.96
sample 6	−53,304.76	0.0953	9575.67	2.53
sample 7	−2409.5	0.217	5,428,526	0.805
sample 8	−364.96	0.483	35.7×10^6	0.494
	K_5	K_6	K_7	K_8
sample 1	1,329,611	1,656,054	39.2	1.733
sample 2	-1.06×10^{11}	1,880,391	79,574.72	1.823
sample 3	-6.05×10^{10}	1,661,827	63,070.94	1.766
sample 4	1,273,710	1,538,259	32.63	4.37
sample 5	-1.43×10^{11}	1,569,176	35,971.7	1.98
sample 6	-2.08×10^{11}	1,676,081	11,647.11	2.42
sample 7	-1.34×10^{11}	2,542,749	1×10^9	0.704
sample 8	-1.32×10^9	4,124,939	298×10^6	0.41

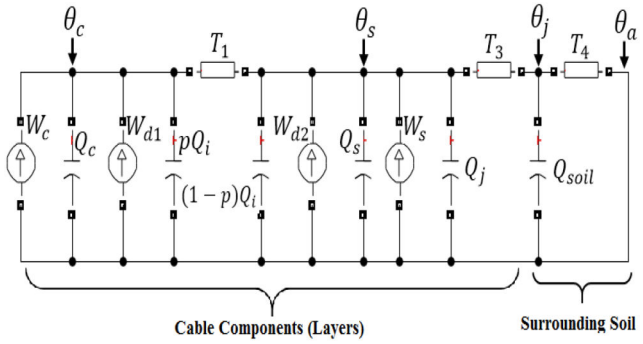

a

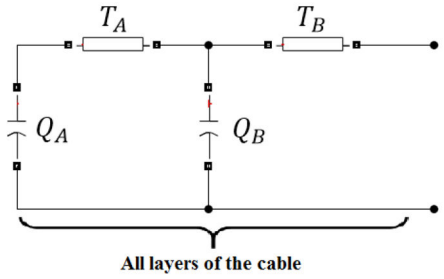

b

Fig. 3 *Thermal circuit of the single-core UGPC and the backfill soil*
(a) Complete thermal circuit of the cable, ***(b)*** Two loops equivalent cable circuit for the dynamic response of IEC 60853-2 thermal circuit of the single-core UGPC and the backfill soil

surrounding soil. Modifications are done to improve its capability for the field conditions simulation during UGPCs load cycling by using (1)–(3). The thermal capacitance and thermal resistance of single-core cable in each cable layer laid in the flat formation and the surrounding soil are calculated by using IEC 60287 and IEC 60853-2 equations [1, 21]

$$T_1 = \frac{\rho_i}{2\pi}\ln\left(\frac{D_i}{d_c}\right) \tag{20}$$

$$T_3 = \frac{\rho_j}{2\pi}\ln\left(\frac{D_e}{D_s}\right) \tag{21}$$

$$T_4 = \frac{\rho_{soil}}{2\pi}\left\{\ln\left(\frac{4L}{D_e}\right) + \ln\left(1 + \left(\frac{2L}{S}\right)^2\right)\right\} \tag{22}$$

$$Q_c = C_{pc} \cdot A_c \tag{23}$$

$$Q_i = \frac{\pi}{4}\left(D_i^2 - d_c^2\right)C_{pi} \tag{24}$$

$$Q_s = \frac{\pi}{4}\left(D_s^2 - D_i^2\right)C_{ps} \tag{25}$$

$$Q_j = \frac{\pi}{4}\left(D_e^2 - D_s^2\right)C_{pj} \tag{26}$$

$$Q_{soil} = \pi\left(L^2 - \left(\frac{D_e}{2}\right)^2\right)C_{psoil} \tag{27}$$

where ρ_i, ρ_j, ρ_{soil}, C_{pc}, C_{pi}, C_{ps}, C_{pj} and C_{psoil} are the thermal resistivity and volumetric specific heat of each cable layer material and the surrounding soil, respectively. Therefore, as it is mentioned before, d_c, D_i, D_s and D_e are the external diametre of the conductor, insulation, screen and the cable surface, respectively. S is the distance between the cables in case of flat formation, L is burial depth and A_c is the cross-sectional area of the conductor. To include the probability of dry zone formation in the backfill soil around the cable during load cycling, (1)–(3) are inserted into the designed program used in the calculations of the dynamic temperature distribution of the cable elements and the surrounding soil during dynamic loading according to IEC 60853-2 which ignored the phenomenon of dry zone formation of the soil.

One way to minimise the dry zone effect that may cause the thermal failure of the cable insulation is to determine the most appropriate mixture of the soil that can be used to fill the blanks around the underground cables [5]. Another way is to reduce the cable current during load cycling for a known time before the surrounding soil of the cable temperature reaches the value that indicates the start of dry zone formation. The flowchart shown in Fig. 4*a* includes suggested algorithm steps to reduce the cable cycle current for specified hours during climax times when the dry zones are started to be formed. The concept is to keep the insulation touching the conductor temperature of the XLPE cable insulation at 85°C which is considered as its operating temperature [29]. This, practically, can be done by inserting thermocouples group along the cable route to measure the surrounding cable temperature and giving the alarm to warn the crew of operation when the dried layers are formed surrounding the cable. The system shown in Fig. 4*b* can be used for this purpose.

The criteria as given in Fig. 4*a* depends on either the soil reaches a state where there is a dry area around the cable or the temperature of the insulator rises to 85°C in either case the current must be reduced to prevent cable insulation breakdown. The monitoring system consists of a number of thermocouples (junction-K) for measuring the temperature and gives the output as the voltage in (mV), signal conditioning circuit with ten times gain can be used for amplifying the output voltage of thermocouples and microcontroller unit containing the program of the flowchart given in Fig. 4*a*, which can be utilised for sending an alarm signal when the temperature exceeds the set point temperature (temperature of dry zone formation).

4 Thermal analysis results and discussion

4.1 Construction details of the 220, 66 and 33 kV cables and their dynamic loading

Load cycles of the cables under study are shown in Fig. 5 through four days.

The cable details and the load cycle are reported by the Egyptian electrical grid company. Details of the 33, 66 and 220 kV cables are given in Table 3. The calculations are carried out when the cables are loaded each by its operating load cycle [33]. The ambient temperature was varied between 0 and 10°C during the night and 24 and 28°C during daylight hours.

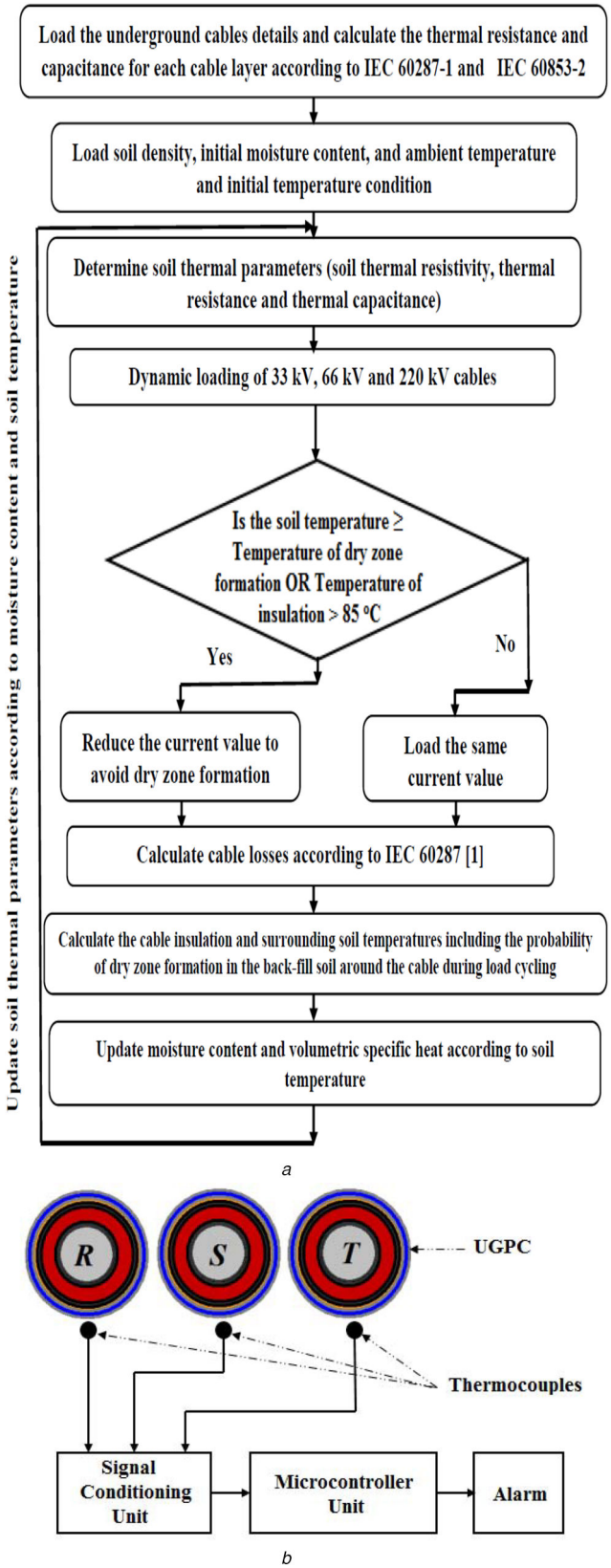

Fig. 4 *Flowchart of suggested modifications on the load cycle and practical system used for the dry zone monitoring*
(a) Flowchart of the suggested modifications on the load cycle, ***(b)*** Practical system used for giving an alarm when the dry zone is formed

4.2 Calculations done on 33 kV, 66 and 220 kV cables and summary of the results

IEC 60853-2 method is used in the calculations of cable insulation and the surrounding soil temperatures. To include the impacts of the soil temperature variations on its thermal resistivity and specific heat, (1)–(3) are incorporated with IEC 60853-2 method.

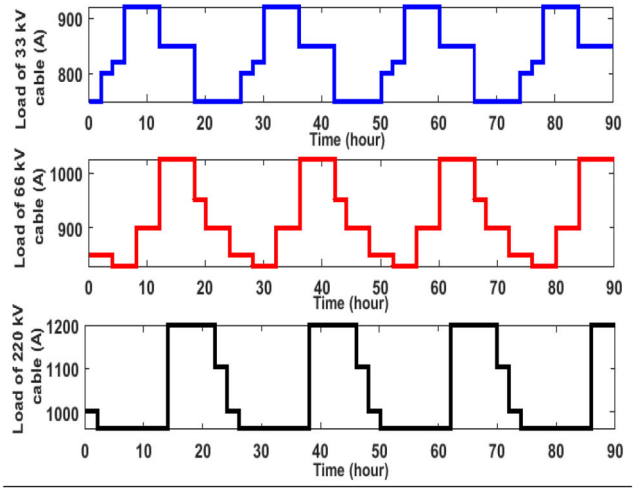

Fig. 5 *Dynamic loading of 33 kV, 66 and 220 kV cables*

Table 3 Construction details of cables understudy

Cables details	220 kV	66 kV	33 kV
conductor material	copper (single core)	copper (single core)	copper (single core)
conductor area, mm^2	1600	1250	1000
conductor diametre, mm	51.9	40	40.2
insulation type	XLPE	XLPE	XLPE
insulation diametre, mm	100.9	65.4	59.5
screen type	copper	copper	aluminium
screen diametre, mm	110.9	73.4	64
cover type	PVC	PVC	PVC
overall cable diametre, mm	121.1	92.3	71

This method is defined as a modified thermoelectric equivalent (MTEE) method. The parameters of these equations for each soil sample are given in Table 2.

Calculations are done to obtain the dynamic temperature of the 33 kV middle cable insulation layer when soil sample 1 is used as backfilling material at full load cycle. As shown in Fig. 6 dry zone is started to be formed after about 62 h from cable loading by its load cycle. The used algorithm suggested reducing the load by 20% after 62 h from starting the cable loading as for 4 h given in case (A). The algorithm recommended as an alternative to reduce the cable's load by 30% after 79 h for 7 h as given in case (B). Figs. 6*a* and *b* give the cable insulation and the soil temperatures of cases A and B. This reduction of the cable loading cycle is done to keep the insulation temperature within the acceptable limit and to minimise the dry zone effect on the cable insulation.

Similar calculations are done on 66 kV cable in case of using surrounding soil sample 1 as backfilling material. The results indicate that the dry band is formed after 72 h as shown in Fig. 7 during full load cable loading. This leads to a rapid increase in insulation temperature. The algorithm given in Fig. 4*a* suggested reducing the cable load by two alternative ways, (A) 20% after 72 h from the cable loading for 2 h or (B) 30% after 83 h from starting of the cable loading for a specified time of 3 h. Figs. 7*a* and *b* show the XLPE insulation and the backfill soil temperatures versus time before and after load cycling corrections, respectively, to minimise dry zone formation effect.

Similar computations are presented when using soil sample 1 as backfill material around 220 kV cable. Figs. 8*a* and *b* show the cable insulation and the backfill soil sample 1 temperatures of the centre phase cable when loaded by its full current cycle. The dry band is formed after 74 h. The proposed algorithm recommended two alternative ways to disconnect the current loading, (A) 20% of the load after 74 h loading for 2 h or (B) 30% of the load after 86 h

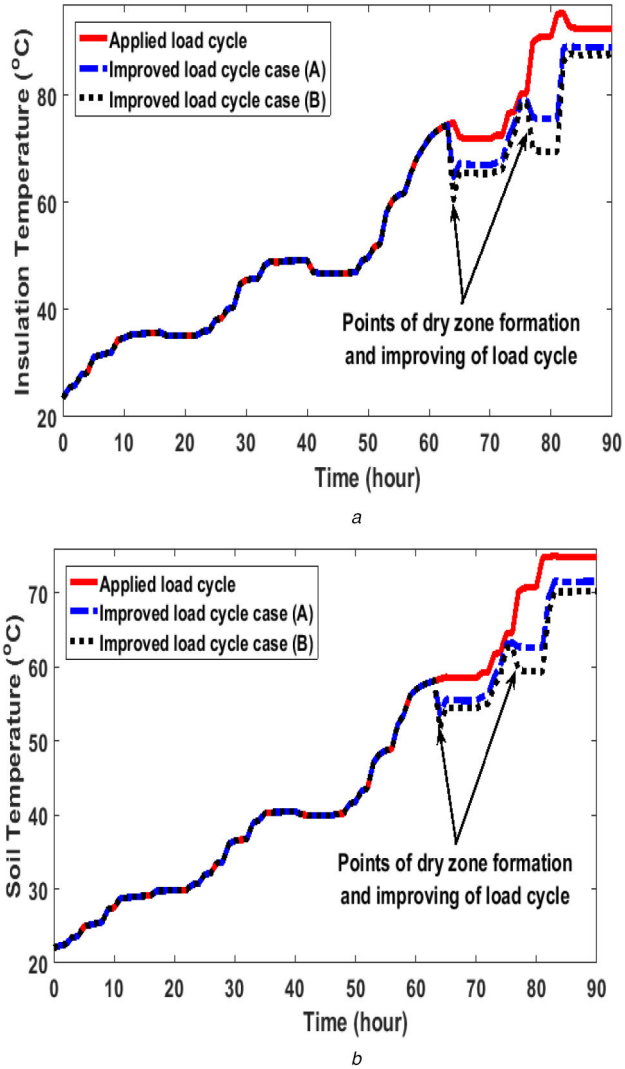

Fig. 6 *Load cycle corrections for 33 kV cable and sample 1 as backfill material*
(a) Insulation, ***(b)*** Soil temperatures

for a specified time of 2 h to protect cable insulation layers from damage. The calculations are carried out during loading the cables each by its operating load cycle [33].

Similar calculations are carried out when soil samples 2, 3, 4, 5, 6 and 7 given in Table 1 are utilised as backfill materials. Summary of the cyclic loading maximum temperatures of the conductor and backfill soil around the cable using the MTEE and IEC 60853-2 technique on 33, 66 and 220 kV cables are given in Tables 4 and 5.

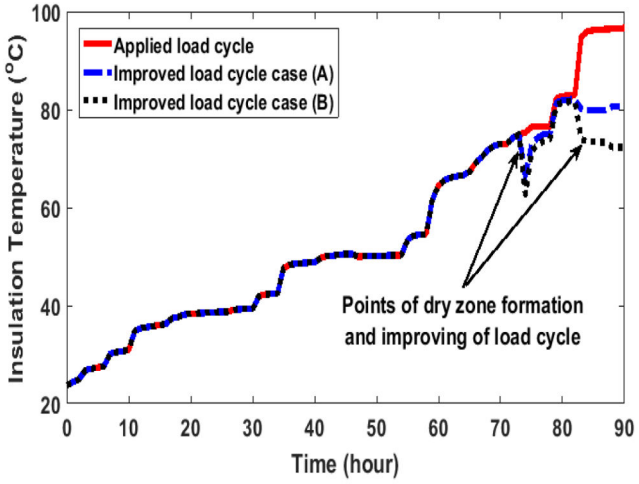

a

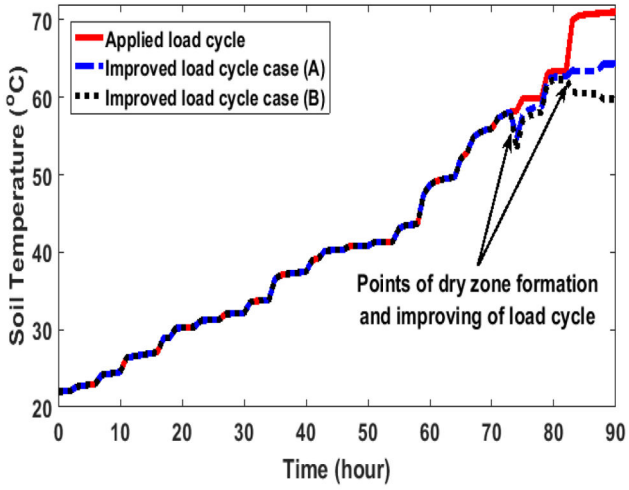

b

Fig. 7 *Load cycle corrections for 66 kV cable and sample 1 as backfill material*
(a) Insulation, ***(b)*** Soil temperatures

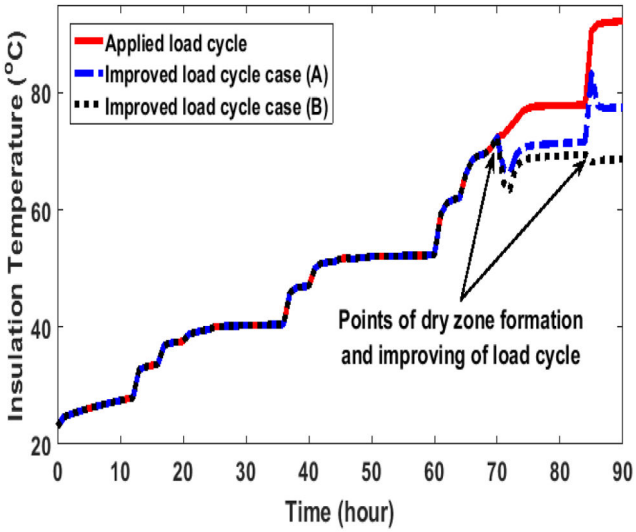

a

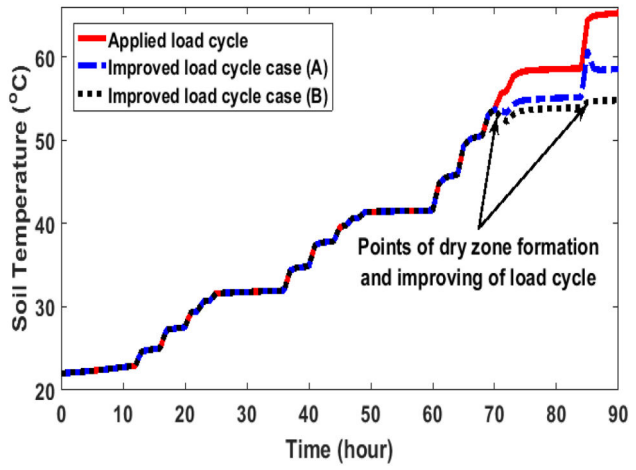

b

Fig. 8 *Load cycle corrections for 220 kV cable and sample 1 as backfill material*
(a) Insulation, ***(b)*** Soil temperatures

Table 4 Summary of 33 and 66 kV cables thermal characteristic buried in the tested soil as backfill materials

Soil sample	33 kV cable			66 kV cable		
	θ_{ct}, °C	θ_{soil}, °C	Time to form dry zone, h	θ_{ct}, °C	θ_{soil}, °C	Time to form dry zone, h
MTEE method						
sample 1	101	75	62	105	72	72
sample 2	90	65	84	101	63	85
sample 3	92	64	82	97	60	84
sample 4	125	91	56	129	84	60
sample 5	131	96	61	135	93	68
sample 6	110	79	81	120	73	82
sample 7	142	99	59	143	90	66
sample 8	58	43	no	63	44	no
IEC 60853-2 method						
sample 1	49	42.5	no	54	46	no
sample 2	47	41	no	53	44	no
sample 3	46	41	no	52	43	no
sample 4	46	41	no	52	43	no
sample 5	46	40	no	52	43	no
sample 6	45	40	no	51	42	no
sample 7	44	39	no	49	41	no
sample 8	43	37	no	48	39	no

θ_{ct} is the conductor temperature.

θ_{soil} is the soil temperature.

Table 5 Summary of 220 kV cable thermal characteristics buried in the tested soil as backfill materials

Soil sample	220 kV cable		
	θ_{ct}, °C	θ_{soil}, °C	Time to form dry zone, h
IEC 60853-2 technique			
sample 1	55	45	No
sample 2	51	41	No
sample 3	51	42	No
sample 4	51	42	No
sample 5	51	42	No
sample 6	50	41	No
sample 7	49	39	No
sample 8	47	37	No
IEC 60853-2 modified technique			
sample 1	86	73	70
sample 2	85	72	87
sample 3	71	61	88
sample 4	90	80	63
sample 5	107	96	65
sample 6	110	99	85
sample 7	112	100	65
sample 8	53	43	no

θ_{ct} is the conductor temperature.

θ_{soil} is the soil temperature.

Table 6 Summary of the 33 kV cable load cycle modifications using the suggested algorithm

Soil samples	θ_{it}, °C	θ_{soil}, °C	Correction of the cable load cycle
1 applied load cycle	93	75	the load cycle is corrected by reducing: (A) 20% of the load after 62 h from starting of load cycle for 4 h or (B) 30% of the load after 79 h of loading for 7 h
improved case (A)	85	68	
improved case (B)	81	65	
2 applied load cycle	83	65	the load cycle is corrected by reducing 20% of load after 84 h of loading for 3 h
improved case (A)	70	53	
3 applied load cycle	84	64	the load cycle is corrected by reducing 20% of the load after 82 h of loading for 4 h
improved case (A)	69	57	
improved case (B)	—	—	
4 applied load cycle	119	91	the load cycle is corrected by reducing: (A) 30% of the load after 56 h of loading for 4 h or (B) 35% of the load after 78 h of loading for 8 h.
improved case (A)	85	67	
improved case (B)	81	64	
5 applied load cycle	123	96	the load cycle is corrected by reducing: (A) 25% of the load after 61 h of loading for 6 h or (B) 30% of the load after 79 h of loading 9 h.
improved case (A)	81	66	
improved case (B)	78	61	
6 applied load cycle	105	79	the load cycle is corrected by reducing: (A) 25% or (B) 30% of the load after 81 h of loading for 5 h
improved case (A)	85	66	
improved case (B)	80	62	
7 applied load cycle	139	99	the load cycle is corrected by reducing: (A) 26% of the load after 60 h of loading for 4 h or (B) 30% of the load after 75 h of loading for 10 h.
improved case (A)	85	67	
improved case (B)	79	63	
8 applied load cycle	52	43	no need to change the load cycle

θ_{it} is the insulation temperature.

θ_{soil} is the soil temperature.

The differences in the conductor and surrounding soil temperatures in case of calculations using IEC60853-2 method from one side and MTEE method from the other side are due to neglecting the influence of temperature and moisture variations during dynamic loads on both the soil thermal capacitance and resistance. For that reason, IEC60853-2 method indicated that no dry band is formed.

Tables 6–8 give a summary of the thermal analysis of the 33, 66 and 220 kV cables, respectively, buried in the tested eight samples as backfilling material surrounding the cable and the recommended modification on the cable loading cycle for each cable type to maintain the insulation temperature at 85°C and not exceeding this limit where the dry zones are formed.

5 Conclusions

The dry zone may be formed around UGPCs due to moisture migration of the soil surrounding the cables. This leads to an increase in the surrounding soil thermal resistivity and rapid increase in the cable insulation temperature causing cable failure. For that reason, an algorithm is suggested in this paper to reduce the cable cycle current for a specified time during climax times, when the dry zones are started to be formed. In this article practical system is proposed for monitoring the dry zone formation around the power cables and to give an alarm when the dry zone is formed.

In the proposed article MTEE is used to study the performance of dry zone formation around the cables used in this study considering eight soil samples as backfill materials. The

Table 7 Summary of the 66 kV cable load cycle modifications using the suggested algorithm

Soil samples	θ_{it}, °C	θ_{soil}, °C	Correction of the cable load cycle
1 applied load cycle	96	72	the load cycle is corrected by reducing: (A) 20% of the load after 72 h for 2 h or (B) 30% of the load after 83 h of loading for 3 h.
improved case (A)	83	64	
improved case (B)	81	63	
2 applied load cycle	91	63	the load cycle is corrected by reducing 10% of the load after 85 h of loading for 2 h
improved case (A)	60	50	
3 applied load cycle	90	60	the load cycle is corrected by reducing: (A) 10% or (B) 15% of the load after 84 h of loading for 2 h
improved case (A)	63	50	
improved case (B)	60	48	
4 applied load cycle	120	84	the load cycle is corrected by reducing: (A) 30% of the load after 60 h of loading for 8 h or (B) 35% of the load after 80 h of loading for 7 h.
improved case (A)	85	64	
improved case (B)	81	61	
5 applied load cycle	126	93	the load cycle is corrected by reducing: (A) 23% of the load after 68 h of loading for 4 h or (B) 27% of the load after 78 h of loading for 10 h
improved case (A)	85	64	
improved case (B)	80	61	
6 applied load cycle	110	73	the load cycle is corrected by reducing: (A) 15% or (B) 20% of the load after 83 h of loading for 4 h
improved case (A)	82	59	
improved case (B)	80	57	
7 applied load cycle	136	90	the load cycle is corrected by reducing: (A) 25% of the load after 66 h of loading for 7 h or (B) 30% of the load after 77 h of loading for 9 h.
improved case (A)	84	61	
improved case (B)	79	60	
8 applied load cycle	55	44	no need to change the load cycle

θ_{it} is the insulation temperature.

θ_{soil} is the soil temperature.

Table 8 Summary of the 220 kV cable load cycle modifications using the suggested algorithm

Soil samples	θ_{it}, °C	θ_{soil}, °C	Correction of the cable load cycle
1 applied load cycle	91	67	the load cycle is corrected by reducing: (A) 20% of the load after 74 h of loading for 3 h or (B) 30% of the load after 86 h of loading for 2 h
improved case (A)	83	61	
improved case (B)	82	55	
2 applied load cycle	82	59	no need to change the load cycle
improved case (A)	—	–	
3 applied load cycle	86	58	the load cycle is corrected by reducing 10% of the load after 86 h of loading for 1 h
improved case (A)	80	56	
improved case (B)	—	—	
4 applied load cycle	112	77	the load cycle is corrected by reducing: (A) 25% of the load after 67 h of loading for 6 h or (B) 30% of the load after 80 h of loading for 5 h
improved case (A)	84	62	
improved case (B)	79	59	
5 applied load cycle	119	80	the load cycle is corrected by reducing: (A) 30% of the load after 70 h of loading for 4 h or (B) 35% of the load after 86 h of loading for 3 h.
improved case (A)	85	62	
improved case (B)	81	60	
6 applied load cycle	112	75	the load cycle is corrected by reducing: (A) 23% of the load after 74 hof loading for 6 h or (B) 27% of the load after 86 h of loading for 4 h
improved case (A)	84	59	
improved case (B)	80	57	
7 applied load cycle	119	74	the load cycle is corrected by reducing: (A) 30% of the load after 71 h of loading for 8 h or (B) 35% of the load after 86 h of loading for 5 h.
improved case (A)	85	60	
improved case (B)	81	59	
8 applied load cycle	56	45	no need to change the load cycle

θ_{it} is the insulation temperature.

θ_{soil} is the soil temperature.

underground power cables insulation and surrounding soil temperatures during load cycling are calculated including the possibility of dry zone formation.

Modifications on the load cycle to keep the insulation temperature within 85°C are suggested to minimise the effect of dry band formation surrounding the XLPE cable on the cable insulation ageing. The thermal analysis of three different cable ratings, single-core cables and the ones installed in the flat formation of 33, 66 and 220 kV cables are presented when buried in different soils as backfill materials.

6 References

[1] IEC publication60287-1-3, : 'Calculations of the continuous current rating of cables (100% load factor)', 1982

[2] Dorison, E., Anders, G. J., Lesur, F.: 'Ampacity calculations for deeply installed cables', *IEEE Trans. Power Deliv.*, 2010, **25**, (2), pp. 524–533

[3] de Leon, F: 'Major factors affecting cable ampacity'. IEEE/Power Engineering Society General Meeting, Montreal, QC, Canada, 18–22 June 2006, paper 06GM0041

[4] Anders, G.J.: '*Rating of electric power cables: ampacity computations for transmission, distribution, and industrial applications*' (IEEE Press, McGraw Hill, 1997)

[5] Gouda, O.E., El Dein, A.Z.: 'Improving underground power distribution capacity using artificial backfill materials', *IET Gener. Transm. Distrib.*, 2015, **9**, (15), pp. 2180–2187
[6] Gouda, O.E., Osman, G.F.A., Salem, W.A.A., *et al.*: 'Load cycling of underground distribution cables including thermal soil resistivity variation with soil temperature and moisture content', *IET Gener. Transm. Distrib.*, 2018, **12**, (18), pp. 4125–4133
[7] Gouda, O.E.: 'Formation of the dried out zone around underground cables loaded by peak loadings', *Model., Simul. Control, ASME Press*, 1986, **7**, (3), pp. 35–46
[8] Gouda, O.E., Osman, G.F.A., Salem, W.A.A., *et al.*: 'Cyclic loading of underground cables including the variations of backfill soil thermal resistivity and specific heat with temperature variation', *IEEE Trans. Power Deliv.*, 2018, **33**, (6), pp. 3122–3129
[9] Gouda, O.E., Amer, G.M., El Dein, A.Z.: 'Improving the under-ground cables ampacity by using artificial backfill materials'. Proc. 14th Int. Middle East Power Systems Conf. (MEPCON'10), Cairo University, Egypt, 19–21 December, 2010, pp. 38–43
[10] Al-Saud, M.S., El-Kady, M.A., Findlay, R.D.: 'Combined simulation-experimental approach to power cable thermal loading assessment', *IET Gener. Transm. Distrib.*, 2008, **2**, (1), pp. 13–21
[11] Ocłon, P., Cisek, P., Pilarczyk, M., *et al.*: 'Numerical simulation of heat dissipation processes in underground power cable system situated in thermal backfill and buried in a multilayered soil', *Energy Convers. Manage.*, 2015, **95**, pp. 352–370
[12] Al-Saud, M.S., El-Kady, M.A., Findlay, R.D.: 'A new approach to underground cable performance assessment', *Electr. Power Syst. Res.*, 2008, **78**, pp. 907–918
[13] de León, F., Anders, G.J.: 'Effects of backfilling on cable ampacity analyzed with the finite element method', *IEEE Trans. Power Deliv.*, 2008, **23**, (2), pp. 537–543
[14] Hegyi, J., Klestoff, A.: 'Current-carrying capability for industrial underground cable installations', *IEEE Trans. Ind. Appl.*, 1988, **24**, (1), pp. 99–105
[15] Hanna, M.A., Chikhani, A.Y., Salama, M.M.A.: 'Thermal analysis of power cables in multi-layered soil, part 3: case of two cables in a trench', *IEEE Trans. Power Deliv.*, 1994, **9**, (1), pp. 572–578
[16] Yenchek, M.R., Cole, G.P.: 'Thermal modelling of portable power cables', *IEEE Trans. Ind. Appl.*, 1997, **33**, (1), pp. 72–79
[17] Anders, G.J., Chaaban, M., Bedard, N., *et al.*: 'New approach to ampacity evaluation of cables in ducts using finite element technique', *IEEE Trans. Power Deliv.*, 1987, **2**, (4), pp. 969–975
[18] El-Kady, M.A., Hydro, O.: 'Calculation of the sensitivity of power cable ampacity to variations of design and environmental parameters', *IEEE Trans. Power Apparatus Syst.*, 1984, **PAS-103**, (8), pp. 2043–2050
[19] Kellow, M.A.: 'A numerical procedure for the calculation of the temperature rise and ampacity of underground cables', *IEEE Trans. Power Appar. Syst.*, 1981, **PAS-100**, (7), pp. 3322–3330
[20] Olsen, R., Anders, G.J., Holboell, J., *et al.*: 'Modelling of dynamic transmission cable temperature considering soil specific heat, thermal resistivity and precipitation', *IEEE Trans. Power Deliv.*, 2013, **28**, (3), pp. 1909–1917
[21] IEC Standard 60853-2: 'Calculation of the cyclic and emergency current ratings of cables, part 2: cyclic rating factor of cables greater than 18/30 (36) kV and emergency ratings for cables of all voltages', Publication 853–862, 1989
[22] Olsen, R.S., Holboell, J., Gudmundsdóttir, U.S.: 'Dynamic temperature estimation and real time emergency rating of transmission cables'. IEEE Power Energy Society General Meeting, San Diego, CA, July 2012, pp. 1–8
[23] Freitas, D.S., Prata, A.T., de Lima, A.J.: 'Thermal performance of underground power cables with constant and cyclic currents in presence of moisture migration in the surrounding soil', *IEEE Trans. Power Deliv.*, 1996, **11**, (3), pp. 1159–1170
[24] Maximov, S., Venegas, V., Guardado, J. L., *et al.*: 'Analysis of underground cable ampacity considering non-uniform soil temperature distributions', *Electr. Power Syst. Res.*, 2016, **132**, pp. 22–29
[25] Zarchi, D.A., Vahidi, B.: 'Optimal placement of underground cables to maximise total ampacity considering cable lifetime', *IET Gener. Transm. Distrib.*, 2016, **10**, (1), pp. 263–269
[26] Carlos, G., Antonio, F.O., José, C.: 'Theoretical model to calculate steady-state and transient ampacity and temperature in buried cables', *IEEE Trans. Power Deliv.*, 2003, **18**, (3), pp. 667–678
[27] Anders, G.J., El-Kady, M.A.: 'Transient ratings of buried power cables part 1: historical perspective and mathematical model', *IEEE Trans. Power Deliv.*, 1992, **7**, (4), pp. 1724–1734
[28] Campbell, G.S., Calissendorff, C., Williams, J.H.: 'Probe for measuring soil specific heat using a heat-pulse method', *Soil Sci. Soc. Am. J.*, 1991, **55**, (1), pp. 291–293
[29] Koopmans, G., Gouda, O.E.: 'Transport of heat and moisture in soils with hysteretic moisture potential'. Proc. Fourth Int. Conf., Swansea, UK, 15–18th July 1985, vol. 2, pp. 846–874
[30] Anders, G.J., Radhakrishna, H.S.: 'Power cable thermal analysis with consideration of heat and moisture transfer in the soil', *IEEE Trans. Power Deliv.*, 1988, **3**, (4), pp. 1280–1288
[31] Donazzi, F., Occhini, E., Seppi, A.: 'Soil thermal and hydrological characteristics in designing underground cables', *Proc. IEE*, 1979, **126**, (6), pp. 506–516
[32] Philip, J.R., De Vries, D.A.: 'Moisture movement in porous materials under temperature gradients', *Trans. Am. Geophysical Union*, 1957, **38**, (2), pp. 222–232
[33] Egyptian Electricity Distribution Companies (EEDC) Reports, 1991–2016